

ACI member **Jun Wang** is a Postdoctoral Associate in the Department of Civil Engineering at the University of Colorado Denver, Denver, CO. She has received BS from Northeast Forestry University, and MS and PhD from the University of Colorado Denver. She is a member of ACI Committee 345 (Concrete Bridge Construction and Preservation). Her research interest includes multi-object interaction and concrete structures.

Yail J. Kim, FACI, is President of the Bridge Engineering Institute, An International Technical Society, and a Professor in the Department of Civil Engineering at the University of Colorado Denver, Denver, CO. He is Chair of ACI Subcommittee 440I (FRP-Prestressed Concrete) and past Chair of ACI Committee 345 (Concrete Bridge Construction and Preservation). He is a member of ACI Committees 342 (Evaluation of Concrete Bridges and Bridge Elements), 377 (Performance-Based Structural Integrity & Resilience of Concrete Structures), 440 (Fiber Reinforced Polymer Reinforcement), and Joint ACI-ASCE Committee 343 (Concrete Bridge Design). He has received the Chester Paul Siess Award for Excellence in Structural Research in 2019. His research interests encompass advanced composite materials for rehabilitation, structural informatics, complex systems, and science-based structural engineering, including statistical, interfacial, and quantum physics.

INTRODUCTION

In the United States, corrosion is considered to be a major problem [1]. Chloride-induced corrosion is responsible for the damage of reinforced concrete structures exposed to marine environments [2]. Since Collepardi et al. [3] adopted Fick's second law for the simulation of chloride migration in concrete, it has been widely used to describe a one-directional chloride diffusion process. The content of chlorides can be determined by analytical equations [4] and the finite difference method [5]. These approaches, however, may not be adequate for practical application when the spatial domain of a concrete member is concerned with the multi-directional movement of chlorides. To address this issue, a two-dimensional cellular automata model may be employed to simulate interactions between neighboring cells in accordance with a given algorithm. The algorithm is utilized iteratively in the time domain of the cells and leads to a solution for a complex problem. Such a modeling technique has been successfully applied to various fields, namely, politics [6], economics [7], transportation [8], and chloride diffusion [9]. The model is capable of simulating a two-dimensional process of chloride migration in reinforced concrete, thereby predicting the corrosion of rebars under corrosive environments. Following a standard of the National Association of Corrosion Engineers (NACE) [10], three corrosive zones may be considered for marine structures: atmospheric, splash, and submerged zones. Chloride-induced corrosion models can be formulated with the process of chloride diffusion in saturated concrete under the atmospheric and submerged conditions, while wet-dry cycles are associated with the splash condition. The wet-dry cycle is a combination of capillary suction and diffusion, which can accelerate corrosion damage [11,12]. Unlike the atmospheric and submerged conditions, where surface chloride concentrations are assumed constant, the surface chloride concentration of concrete subjected to splash increases over time [13]. This paper deals with a preliminary study concerning the applicability of cellular automata in simulating a corrosion process in a bridge column subjected to those marine environments. Upon verifying the modeling concept, follow-up research will be carried out and refined outcomes will be reported in due course.

RESEARCH SIGNIFICANCE

Because of socioeconomic concerns caused by the corrosion of reinforced concrete, an adequate understanding of chloride-induced corrosion is imperative. A cellular automata model is developed to predict the consequences of corrosion damage in a concrete column under marine environments.

BENCHMARK BRIDGE

A bridge column is designed per the American Association of State Highway Transportation Officials (AASHTO) Load and Resistance Factor Design (LRFD) Bridge Design Specifications (BDS) [14]. Its constituent materials and structure are presented in this section. Corrosive environments that affect the performance of the column are also discussed.

Materials

The column concrete had a strength of $f'_c = 30$ MPa (4,350 psi) at a water-cement-ratio ratio of $w/c = 0.54$ based on ACI 211.1-91 [15]. The ingredients were water (193 kg/m³ (12.05 lb/ft³)), cement (358 kg/m³ (22.35 lb/ft³)), coarse aggregate (1,144 kg/m³ (71.42 lb/ft³)), and fine aggregate (679 kg/m³ (42.39 lb/ft³)). The yield strength and elastic modulus of reinforcing steel were $f_y = 414$ MPa (60 ksi) and $E_s = 200$ GPa (29,000 ksi), respectively.

Structural Description

The circular tied column was reinforced with twelve No. 14 rebars (diameter: $\phi = 43$ mm (1.69 in.) and cross-sectional area: $A_s = 1,452$ mm² (2.25 in.²), each). Complying with AASHTO LRFD BDS [14], a concrete cover of 125 mm (4.92 in.) was assigned for a direct exposure to saltwater.

Service Environments

As stated in the NACE standard [10], three service environments were involved: atmospheric, splash, and submerged zones.

MODELING

An evolutionary modeling approach is described with the principle of chloride diffusion, multi-agent interaction, and corrosion initiation.

Cellular Automata Model

Modeling program—A cellular automata algorithm was programmed using an agent-based modeling platform, *NetLogo* [16,17]. The software provides a two-dimensional space comprising a grid of square agents, representing constituent materials. Individual agents interacted with their surrounding environments, as explained below.

Interaction rule—Fick's second law was used to simulate interactions between adjacent agents ([4],[18],[19])

$$\frac{\partial C}{\partial t} = D_{ce}(t) \frac{\partial^2 C}{\partial x^2} \quad (1)$$

where C is the chloride content; $D_{ce}(t)$ is the chloride diffusion coefficient in concrete at time t ; and x is the diffusion depth. The differential equation was approximated by the cellular automata algorithm [9]. The local rule used by the model for the simulation of chloride diffusion is presented in Eq. 2, showing that chlorides migrate in both vertical and horizontal directions. Figure 1(a) presents a sectional model for the column surrounded by an environment. The progression of chloride contents ($C_{center,t+1}$) was determined (Eq. 2), as depicted in Fig. 1(b) with $\phi_6 = (1 - \phi_1)/4$ [20]

$$C_{center,t+1} = \phi_1 C_{center,t} + \phi_2 C_{north,t} + \phi_3 C_{east,t} + \phi_4 C_{south,t} + \phi_5 C_{west,t} \quad (2)$$

where $C_{center,t}$ is the chloride concentration in the center agent at current time step t ; $C_{north,t}$, $C_{east,t}$, $C_{south,t}$, and, $C_{west,t}$ are the chloride contents in the neighboring agents; and ϕ_i ($i = 1,2,3,4$, and 5) is the evolutionary coefficient that satisfies Eq. 3 [9].

$$\sum \phi_i = 1 \quad (3)$$

It was assumed that concrete was an isotropic media [21]; as a result, the evolutionary coefficients of the four neighboring agents were equal. In other words, the probabilities of chloride diffusion toward the four directions were identical: $\phi_2 = \phi_3 = \phi_4 = \phi_5$. Podrouzek and Tepy [20] found that the accuracy of the model would be adequate when $\phi_1 = 0.5$, and ϕ_i ($i = 2,3,4$, and 5) = 0.125. As shown in Eq. 4, ϕ_1 had a typical relationship with the chloride diffusion coefficient ($D_{ce}(t)$) [20].

$$\Delta t = \phi_1 \frac{\Delta x^2}{D_{ce}(t)} \quad (4)$$

where Δx and Δt are the size of the agent and the time step, respectively. The diffusion coefficient at the first year $D_{ce}(1)$ (mm²/year) was figured out with the water-to-cement ratio and exposure environments [22]

$$D_{ce}(1) = k_D \times \exp\left(-\frac{10}{\sqrt{eqv(w/c_D)}}\right) \quad (5)$$

$$eqv(w/c_D) = \frac{W}{PC+FA+7 \times SF} \quad (6)$$

where k_D is a factor based on service environment ($k_D = 10,000 \text{ mm}^2/\text{year}$ ($15.5 \text{ in}^2/\text{year}$) for the atmospheric condition, $k_D = 15,000 \text{ mm}^2/\text{year}$ ($23.25 \text{ in}^2/\text{year}$) for the splash condition, and $k_D = 25,000 \text{ mm}^2/\text{year}$ ($38.75 \text{ in}^2/\text{year}$) for the submerged condition [22]; and W , PC , FA , and SF represent the mass of water, portland cement, fly ash, and silica fume, respectively. The equivalent w/c_D ratio (Eq. 6) was equal to the water-to-cement ratio because only portland cement was involved as a cementitious material in this study. To appraise the time-dependent property of the diffusion coefficient $D_{ce}(t)$, a power function was used [23]

$$D_{ce}(t) = D_{ce}(1)t^{-\alpha} \quad (7)$$

$$\alpha = k_\alpha (1 - 1.5 \times eqv(w/c_D)) \quad (8)$$

where $D_{ce}(1)$ is the diffusion coefficient (mm^2/year) at the first year; α is the age parameter to consider the time-dependent diffusion coefficient; and k_α is a factor depending upon exposure condition ($k_\alpha = 1$ for the atmospheric condition; $k_\alpha = 0.1$ for the splash condition; and $k_\alpha = 0.6$ for the submerged condition [22]).

Boundary condition—To approximate the circular shape of the column in a simulation space, over 164,000 agents were necessary ($4 \times 4 \text{ mm}$ ($0.16 \times 0.16 \text{ in.}$), each). Figure 2 compares chloride distributions with various agent sizes when the time and environment were 10 years and the submerged condition, respectively. The sensitivity analysis indicated that the convergence of the chloride distribution was obtained at an agent size of 8 mm (0.31 in.) and smaller. Similar observations were found in other cases when the time and environment were changed.

Simulation—One-dimensional models were prevalent to simulate chloride migration, which can only handle chloride distributions in a single direction. In practice, chloride contents are determined by the interaction of multidirectional agents [24]. Therefore, it was necessary to develop a two-dimensional model for the column. The views of chloride migration from 1 year to 100 years are illustrated in Fig. 3.

Validation—A comparison between predicted chloride concentrations and those provided by literature [25] is presented in Fig. 4. The surface chloride concentration and diffusion coefficient given in Cao et al. [25] were 0.5% of concrete weight and $3.22 \times 10^{-12} \text{ m}^2/\text{s}$ ($4.99 \times 10^{-8} \text{ in.}^2/\text{s}$), respectively, and their approach was independently assessed by others [26].

Corrosion—The corrosion initiation year (t_i) of the column under the atmospheric and submerged conditions is estimated by [27]

$$t_i = \frac{(c/10)^2}{4D_{ce}(1)} \left[\text{erf}^{-1} \left(\frac{C_{cr} - C_0}{C_i - C_0} \right) \right]^2 \quad (9)$$

where c is the concrete cover in mm; erf is the Gauss error function; C_{cr} is the critical chloride concentration ($C_{cr} = 0.4\%$ of cement weight [28]); C_i is the initial chloride content that is assumed to be 0% of the cement weight [28]; and C_0 is the surface chloride content (0.2% and 0.5% of concrete weight under the atmospheric and submerged conditions, respectively [29]). The corrosion current density (i_{corr} in $\mu\text{A}/\text{cm}^2$) was determined using [30]

$$\ln(1.08 i_{corr}(t)) = 8.37 + 0.618 \ln 1.69 C_f(t) - 3034/T - 0.000105 R_c + 2.32t^{-0.215} \quad (10)$$

where T is the temperature at the steel surface in Kelvin ($T = 293.15\text{K}$); R_c is the resistance of the concrete cover in ohms ($R_c = 1,500 \text{ Ohms}$); t is the exposure time in year; and $C_f(t)$ is the free chloride concentration in kg/m^3 , which may be determined by [31]

$$C_f(t) = 0.8541 C_t(t) \quad (11)$$

where $C_t(t)$ is the total chloride concentration attained from the cellular automata model in kg/m^3 . The chloride concentration of the concrete under the atmospheric and submerged conditions were constant; however, a power equation was used for the splash condition ($C_0(t)$ in % weight of concrete) [32]

$$C_0(t) = [0.213 \left(\frac{w}{c}\right) + 0.134]t^{0.484} \quad (12)$$

where $\frac{w}{c}$ is the water to cement ratio and t is the exposure time in years. Because the surface chloride contents of the splash case increases significantly ($C_0(t) > C_0$), a corrosion initiation year predicted by Eq. 9 needs to be adjusted. A threshold current density of $i_{corr} = 0.3 \mu A/cm^2$ ($1.94 \mu A/in.^2$) was employed to predict the corrosion initiation year under the splash condition [33] by converting Eq. 10

$$t_i = \left(\frac{\ln(1.08 \times 0.3) - 8.37 - 0.618 \ln 1.69 C_f(t) + \frac{3034}{T} + 0.000105 R_c}{2.32} \right)^{0.215} \quad (13)$$

Val and Melcher [34] proposed an equation for a reduction in the diameter of rebars when t is larger than t_i

$$d_b(t) = d_b - 0.0232 \int_{t_i}^t i_{corr}(t) dt \quad (14)$$

where $d_b(t)$ is the rebar diameter at year t and d_b is the initial rebar diameter. The analytical expression was approximated to be

$$d_b(t) = d_b - \sum_{t=0}^{t=100} 0.0232 i_{corr}(t) \Delta t \quad (15)$$

Table 1 summarizes the modeling parameters used for the present simulation.

SIMULATION RESULTS

The migration of chlorides is computed under various exposure conditions to predict chloride concentrations, corrosion current density, and a reduction in rebar diameter.

Diffusion—Fig. 5 illustrates the diffusion coefficients of chlorides for the concrete subjected to the corrosive environments. In all cases the diffusion coefficients decreased exponentially over time, which were ascribed to the changes in the pore structure of the concrete [35, 36]. The submerged condition resulted in the highest diffusion coefficient, followed by the splash and atmospheric conditions. A similar trend was reported by others [29].

Chloride concentration—Fig. 6 presents the increased chloride concentrations of the concrete at the steel-surface level over time. During the early years, the chloride concentration of the submerged case was higher than that of the splash case due to the former's higher surface chloride concentration and diffusion coefficient (Table 1). When the time reached 20 years, the chloride concentration of the splash case exceeded the submerged case, resulting from the effects of wet-dry cycles. This observation agrees with the findings of 10-year experimental results [37]: chloride concentrations in a submerged zone were higher than the concentration in a splash zone for the first five years; however, the chloride concentration of the splash case developed significantly after five years compared with that of the submerged zone. The chloride concentration of the atmospheric case was consistently lower because the concrete was exposed to air-borne chlorides. Figure 7 presents a decreasing trend in the chloride concentrations at 100 years. The splash condition exhibited higher chloride concentrations than the submerged and atmospheric conditions.

Corrosion current density—Ferrous ions from the reinforcing steel reacted with oxygen and water [38]. As shown in Fig. 8, regardless of the environment, the corrosion current density of the column gradually slowed down with the accumulation of rust [39]. Among the three environments, the splash condition had the highest corrosion current density because of the expedited corrosion environment with sufficient oxygen, chlorides, and electrolytes.

Reduction in rebar diameter—A reduction in the diameter of the reinforcing bars occurred when the exposure time reached a corrosion initiation year. As shown in Fig. 9, the corrosion initiation year in the splash zone was similar to the year in the submerged zone with a 7% difference; on other hand, the initiation year of the atmospheric case was remarkably higher than others. Consequently, the reduced rebar diameter under the atmospheric condition was lower than the reduction under the splash and submerged conditions (Fig. 10). The amount of reductions under the submerged condition was larger compared with the amount under the splash condition at early years owing to its higher surface chloride content and diffusion coefficient, whereas the reduction in the splash condition exceeded the submerged case after 40 years because of the wet-dry influence in the splash zone.

CONCLUDING REMARKS

This preliminary research has examined the chloride migration of a bridge column under atmospheric, splash, and submerged conditions, based on a cellular automata model, which led to the development of corrosion current density and a reduction in the diameter of reinforcing bars. The following conclusions are drawn:

- The splash condition showed higher chloride concentrations at the surface of the rebar than the submerged and atmospheric conditions; accordingly, the corrosion current density of the column concrete under the splash condition was greater with a larger reduction in the rebar diameter.
- The corrosion initiation year of the column under the splash and submerged conditions was analogous; however, the initiation year under the atmospheric condition was lower than others.

The ongoing research includes an investigation into the consequences of variable concrete mixtures and construction methods, the behavior of the corroded column subjected to axial compression combined with flexural loading, and the efficacy of composite-based rehabilitation.

ACKNOWLEDGMENTS

The authors would like to acknowledge support from the US Department of Transportation through the National Center for Transportation Infrastructure Durability & Life-Extension (TriDurLE).

REFERENCES

- [1] Koch, G.H., Brongers, M.P.H., Thompson, N.G., Virmani, Y.P., and Payer, J.H. 2002. Corrosion cost and preventive strategies in the United States, FHWA-RD-01-156, U.S. Department of Transportation, Federal Highway Administration, Washington D.C.
- [2] Morris, W., Vico, A., and Vazquez, M. 2004. Chloride induced corrosion of reinforcing steel evaluated by concrete resistivity measurements, *Electrochimica Acta*, 49(25), 4447-4453.
- [3] Collepardi, M., Marcialis, A., and Turrizzani, R. 1970. The kinetics of diffusion of chloride ions into the concrete, *Journal of the American Ceramic Society*, 67(4), 157-164.
- [4] Costa, A. and Appleton, J. 1999. Chloride penetration into concrete in marine environment - part II: prediction of long term chloride penetration. *Materials and Structures*, 32(219), 354-59.
- [5] Funahashi, M. 1990. Predicting corrosion free service life of a structure in a chloride environment, *ACI Materials Journal*, 87(6), 581-587.
- [6] Alves, S., Neto, N., and Martins, M. 2002. Electoral survey's influence on the voting processes: a cellular automata model, *Physica A: Statistical Mechanics and its Applications*, 316(1-4), 601-614.
- [7] Fan, Y., Ying, S., Wang, B., and Wei, Y. 2009. The effect of investor psychology on the complexity of stock market: an analysis based on cellular automaton model, *Computers & Industrial Engineering*, 56(1), 63-69.
- [8] Darbha, S., Rajagopal, K., and Tyagi, V. 2008. A review of mathematical models for the flow of traffic and some recent results, *Nonlinear Analysis: Theory, Methods & Applications*, 69(3), 950-970.
- [9] Biondini, F., Bontempi, F., Frangopol, D.M., and Malerba. 2004. Cellular automata approach to durability analysis of concrete structures in aggressive environments. *Journal of Structural Engineering*, 130(11), 1724-1737.
- [10] NACE. 2003. Corrosion control of steel fixed offshore structures associated with petroleum production, NACE RP0176. NACE International.
- [11] Bastidas-Arteaga, E., Sanchez-Silva, M., Chateauneuf, A., and Silva, M.R. 2008. Coupled reliability model of biodeterioration, chloride ingress and cracking for reinforced concrete structures, *Structural Safety*, 30(2), 110-129.
- [12] Gao, J., Yu, Z., Song, L., Wang, T., and Wei, S., 2013. Durability of concrete exposed to sulfate attack under flexural loading and drying-wetting cycles. *Construction and Building Materials*, 39, 33-38.

- [13] Song, H.W., Chang, H.L., and Ann, K.Y. 2008. Factors influencing chloride transport in concrete structures exposed to marine environments. *Cement and Concrete Composites*, 30(2): 113-121.
- [14] AASHTO. 2020. AASHTO LRFD bridge design specifications (9th edition), American Association of State Highway Transportation Officials, Washington, D.C.
- [15] ACI. 2002. Standard practice for selecting proportions for normal, heavyweight, and mass concrete (ACI 211.1-91: reapproved 2002), American Concrete Institute, Farmington Hills, MI.
- [16] Wilensky, U. 1999. NetLogo, Center for Connected Learning and Computer-Based Modeling, Northwestern University, Evanston, IL.
- [17] Wilensky, U. and Rand, W. An introduction to agent-based modeling, The MIT Press, Boston, MA.
- [18] Tuutti, K. 1982. Corrosion of steel in concrete, Swedish Cement and Concrete Research Institute.
- [19] Tang, L., and Joost, G. 2007. On the mathematics of time-dependent apparent chloride diffusion coefficient in concrete, *Cement and Concrete Research*, 37(4), 589-595.
- [20] Podrouzek, J, and Tepy, B. 2008. Modelling of chloride transport in concrete by cellular automata, *Engineering Mechanics*, 15(3), 213-222.
- [21] Wang, Y., An, M., Yu, Z., Han, B., and Ji, W. 2018. Experimental and cellular-automata-based analysis of chloride ion diffusion in reactive powder concrete subjected to freeze–thaw cycling, *Construction and Building Materials*, 172, 760-769.
- [22] Frederiksen, J.M., Mejlbro, L., and Poulsen, E. 2000. The HETEK model of chloride ingress into concrete made simpler by approximations, *Second International RILEM Workshop on Testing and Modelling the Chloride Ingress into Concrete*, RILEM Publications SARL, 317-336.
- [23] Poulsen, E. and Mejlbro, L. 2019. Diffusion of chloride in concrete: theory and application, CRC Press, Boca Raton, FL.
- [24] Val, D.V. and Trapper, P.A. 2008. Probabilistic evaluation of initiation time of chloride-induced corrosion, *Reliability Engineering and System Safety*, 93(3), 364-372.
- [25] Cao, J., Wang, Y., Li, K., and Ma, Y. 2012. Modeling the diffusion of chloride ion in concrete using cellular automaton, *Journal of Materials in Civil Engineering*, 24 (6), 783-788.
- [26] Chatterji, S. 1995. On the applicability of Fick's second law to chloride ion migration through portland cement concrete, *Cement and Concrete Research*, 25(2), 299-303.
- [27] Thoft-Christensen, P., Jensen, F.M., Middleton, C.R., and Blackmore, A. 1996. Assessment of the reliability of concrete slab bridges, 7th IFIP WG 7.5 Working Conference, Boulder, CO, 1-8.
- [28] Elsener, B. and Angst, U. 2016. Corrosion inhibitors for reinforced concrete, *Science and Technology of Concrete Admixtures*, 321-339.
- [29] Roy, S.K., Chye, L.K., and Northwood, D.O. 1993. Chloride ingress in concrete as measured by field exposure tests in the atmospheric, tidal and submerged zones of a tropical marine environment, *Cement and Concrete Research*, 23(6), 1289-1306.
- [30] Liu, T. and Weyers, R.W. 1998. Modeling the dynamic corrosion process in chloride contaminated concrete structures, *Cement and Concrete Research*, 28(3), 365-379.

- [31] Cheewaket, T., Jaturapitakkul, C and Chalee, W. 2010. Long term performance of chloride binding capacity in fly ash concrete in a marine environment, *Construction and Building Materials*, 24(8), 1352-1357.
- [32] Liu, Q., Hu, Z., Lu, X., Yang, J., Azim, I., and Sun, W. 2020. Prediction of chloride distribution for offshore concrete based on statistical analysis, *Materials*, 13(1), 174, 16 pp.
- [33] Yoon, S., Wang, K., Weiss, W.J., and Shah, S.P. 2000. Interaction between loading, corrosion, and serviceability of reinforced concrete. *ACI Materials Journal*, 97(6), 637-644.
- [34] Val, D.M. and Melchers, R.E. 1997. Reliability of deteriorating RC slab bridges, *Journal of Structural Engineering*, 123(12), 1638-1644.
- [35] Maage, M., Helland, S., Poulsen, E., Vennesland, O., and Carlsen, J.E. 1996. Service life prediction of existing concrete structures exposed to marine environment, *ACI Materials Journal*, 93(6), 1-8.
- [36] Yu, Z., Ma, J., Ye, G. van Breugel, K., and Shen, X. 2017. Effect of fly ash on the pore structure of cement paste under a curing period of 3 years, *Construction and Building Materials*, 144, 493-501.
- [37] Tang, L. 2003. Chloride ingress in concrete exposed to marine environment-field data up to 10 years exposure, SP Report 2003:16, SP Swedish National Testing and Research Institute, Boras, Sweden.
- [38] Gaidis, J.M. 2004. Chemistry of corrosion inhibitors, *Cement and Concrete Composites*, 26(3), 181-189.
- [39] Yuan, Y., Jiang, J., and Peng, T. 2010. Corrosion process of steel bar in concrete in full lifetime, *ACI Materials Journal*, 107(6), 562-567.

Table 1—Modeling parameters [1 MPa = 145 psi; 1 mm = 0.0394 in.; 1 m = 3.28 ft]

Service environment	Diffusion coefficient $D_{ce}(1)$ ($\times 10^{-12}$ m ² /s)	Age parameter α	Surface chloride concentration C_1 (% wt. of cement)	Corrosion initiation t_i (year)
Atmospheric	4.29	0.19	1.33	54.1
Splash	6.43	0.019	$1.65t^{0.484}$	8.97
Submerged	10.72	0.114	3.31	9.6

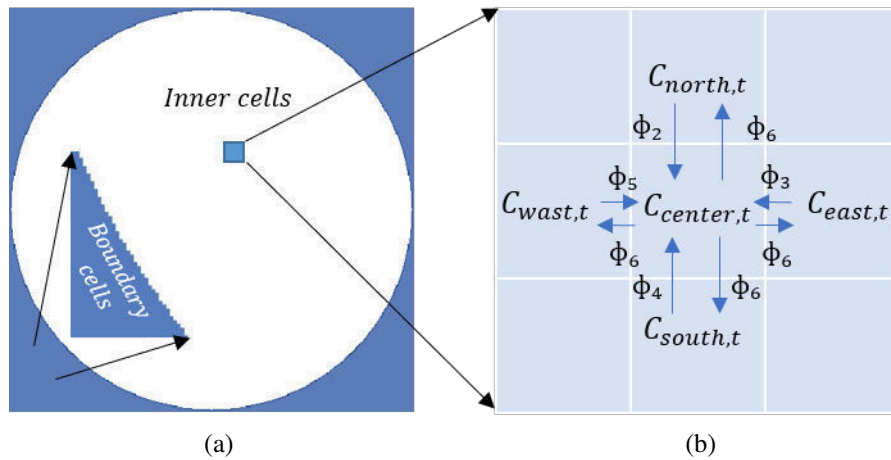


Fig. 1—Concept of two-dimensional cellular automata model: (a) column cross section; (b) interaction

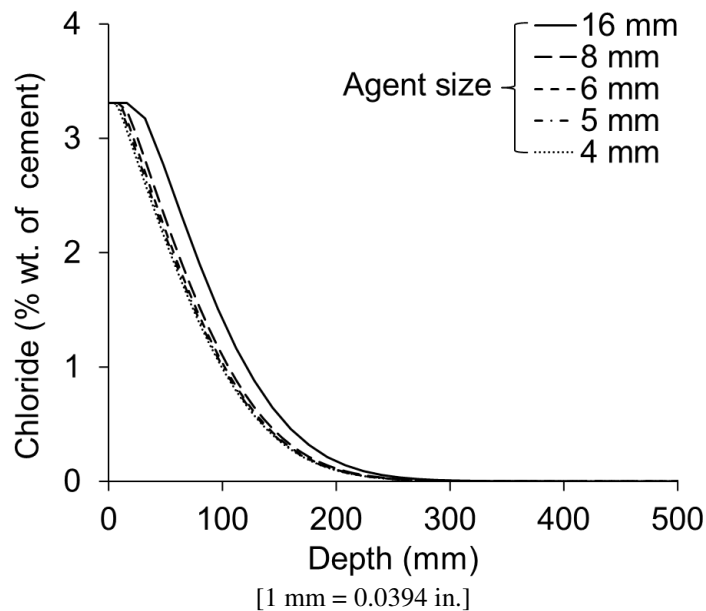


Fig. 2—Convergence of chloride concentration

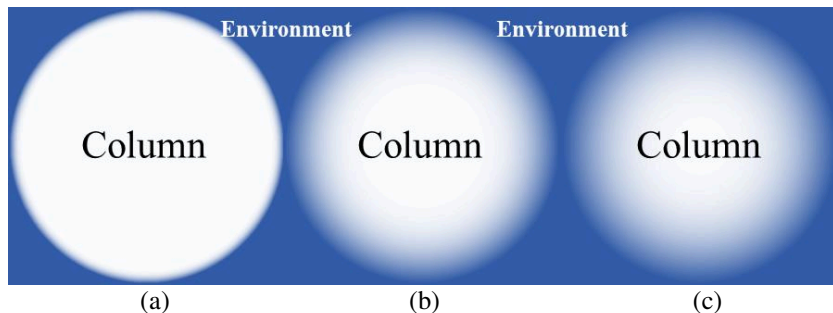


Fig. 3—Chloride migration in column concrete over time: (a) 1 year; (b) 50 years; (c) 100 years

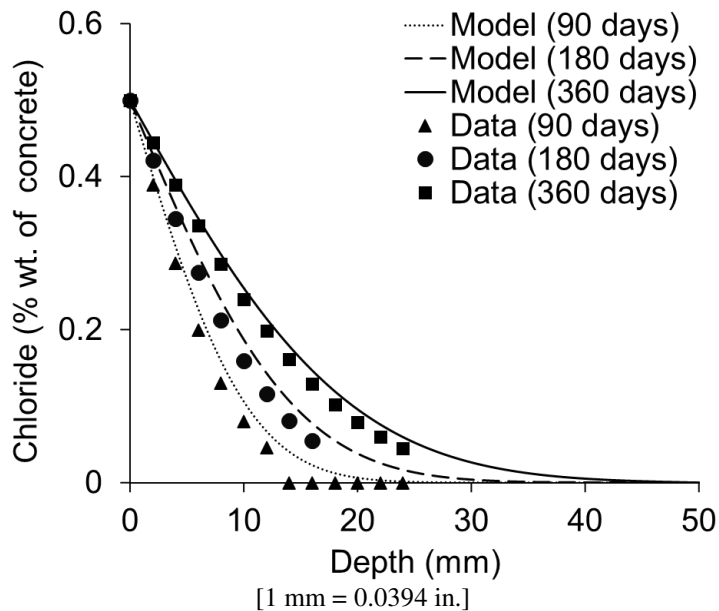


Fig. 4—Validation of the model

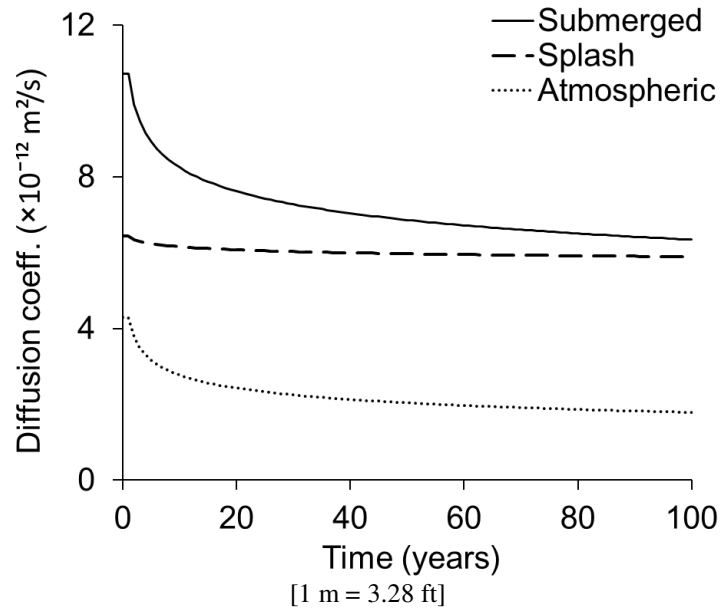


Fig. 5—Comparison of time-dependent diffusion coefficients under various service environments

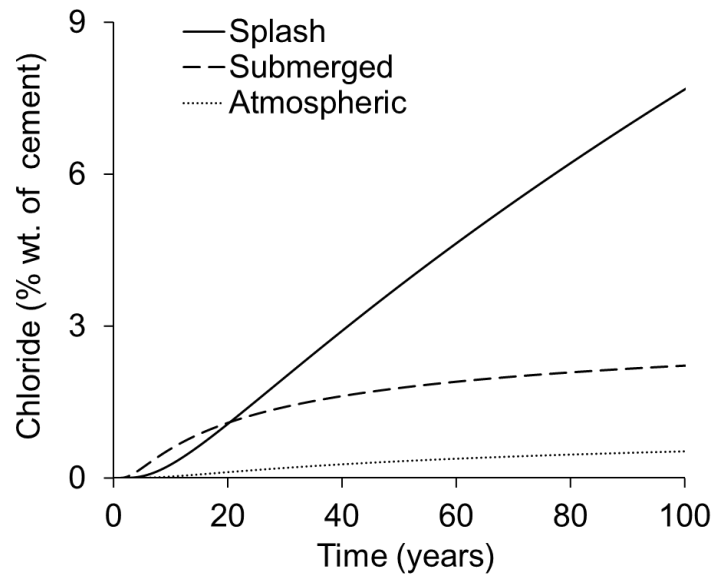


Fig. 6—Chloride concentration at steel surface level subjected to different service environments